Available online at www.sciencedirect.com
ScienceDirect
Polymer 49 (2008) 2243–2252
polymer
www.elsevier.com/locate/polymer

Synthesis and crosslinking of partially disulfonated poly(arylene ether sulfone) random copolymers as candidates for chlorine resistant reverse osmosis membranes

Mou Paul [a], Ho Bum Park [b], Benny D. Freeman [b], Abhishek Roy [a], James E. McGrath [a], J.S. Riffle [a,*]

[a] *Macromolecules and Interfaces Institute, Virginia Polytechnic Institute and State University, Blacksburg, VA 24061, USA*
[b] *Department of Chemical Engineering, Center for Energy and Environmental Resources, University of Texas at Austin, Austin, TX 78758, USA*

Received 18 October 2007; received in revised form 19 February 2008; accepted 23 February 2008
Available online 29 February 2008

Abstract

Biphenol-based, partially disulfonated poly(arylene ether sulfone)s synthesized by direct copolymerization show promise as potential reverse osmosis membranes. They have excellent chlorine resistance over a wide range of pHs and good anti-protein and anti-oily water fouling behavior. Crosslinking of these copolymers that have high degrees of disulfonation may improve salt rejection of the membranes for reverse osmosis performance. A series of controlled molecular weight, phenoxide-endcapped, 50% disulfonated poly(arylene ether sulfone)s were synthesized. The copolymers were reacted with a multifunctional epoxy resin and crosslinked thermally. The effects on network properties of various factors such as crosslinking time, copolymer molecular weight and epoxy concentration were investigated. The crosslinked membranes were characterized in terms of gel fraction, water uptake, swelling and self-diffusion coefficients of water. The salt rejection of the cured membranes was significantly higher than that for the uncrosslinked copolymer precursors.

Keywords: Membrane; Disulfonated poly(arylene ether sulfone); Reverse osmosis

1. Introduction

In recent years, there has been an increasing worldwide need for fresh drinking water [1]. About 41% of the total population in the world lives in water-stressed areas. Membrane technology for desalination, such as reverse osmosis (RO), is an attractive and energy efficient way to develop new sources of fresh water [2]. Over the last four decades, tremendous research has been conducted to develop RO membranes. However, there have been severe gaps in achieving ideal performance. One of the major issues is the chlorine instability of polyamide (PA) RO membranes, which are the most widely used desalination membranes. RO membranes are often exposed to low levels of chorine to prevent biofouling [3]. Unfortunately, the conventional aromatic PA thin film composite membrane is susceptible to oxidative degradation by chlorine, and this leads to irreversible performance loss over time [4–6]. This problem necessitates the use of expensive dechlorination and rechlorination treatment steps when using PA membranes.

Sulfonated poly(arylene ether sulfone)s are promising chlorine resistant RO materials. Unlike commercial aromatic PA membranes, sulfonated poly(arylene ether sulfone)s do not possess the vulnerable amide bond that is susceptible to chlorine attack [7,8]. The use of sulfonated aromatic polymers as RO membranes began with sulfonated poly(phenylene oxide) in 1970s [9]. The sulfonate ions on the polymer repel like charges (the anions from the salt in solution) and as a result, the membrane is relatively impermeable to salts. These

* Corresponding author. Virginia Polytechnic Institute and State University, Macromolecules and Interfaces Institute, Department of Chemistry, Davidson Hall, Blacksburg, VA 24061-0211, USA. Tel.: +1 540 231 6717; fax: +1 540 231 8517.
E-mail address: judyriffle@aol.com (J.S. Riffle).

0032-3861/$ - see front matter © 2008 Elsevier Ltd. All rights reserved.
doi:10.1016/j.polymer.2008.02.039

membranes showed excellent resistance against compaction, hydrolysis and degradation and exhibited good flux and rejection characteristics [10]. Sulfonated poly(arylene ether sulfone) membranes have also been considered for RO applications [11,12]. Albany International Corporation reported sulfonated polysulfone hollow fiber membranes with constant flux and salt rejection even after exposure to 100 ppm chlorine in feed water [13]. However, all of these membranes were post-sulfonated (after the non-sulfonated poly(arylene ether sulfone) was prepared) using chlorosulfonic acid or concentrated sulfuric acid, and undesirable side reactions as well as poor quantitative reproducibility were encountered [14].

Recently, we have described direct copolymerization synthesis of sulfonated biphenol-based poly(arylene ether sulfone)s (BPS) using disulfonated activated aromatic halide monomers [15–23]. These aromatic, film-forming copolymers have well-controlled ion concentrations with excellent oxidative, hydrolytic and mechanical stability. Membranes fabricated from these copolymers have excellent chlorine resistance over a pH range of 4–10. For example, BPS with 40% disulfonation and a commercial PA RO membrane were exposed to feed water containing 500 ppm chlorine at a pH of 9.5. The salt rejection of the PA membrane decreased by 20% after only 20 h of exposure and it continued to decrease rapidly. In contrast, the BPS membrane showed no significant change in salt rejection, and this clearly demonstrates its excellent chlorine tolerance relative to conventional desalination membranes [24–26]. These polymers also exhibit low fouling in oily or protein contaminated water, and high water flux with moderate salt rejection.

In general for these copolymers, water permeability increases and salt rejection decreases with increasing degree of disulfonation [22]. At high ion concentrations, the membranes swell strongly in water, leading to a loss in mechanical stability and ion rejection. Crosslinking such membranes is one approach for reducing the swelling of these membranes and improving their mechanical stability without significantly impairing water flux. Strategies for crosslinking sulfonated polysulfones include van der Waals interactions, hydrogen bonding, ionic or covalent crosslinking, and forming composite blends [27]. Covalent crosslinking has the most pronounced effect on the polymer structure because it permanently fixes the morphology of the polymer. In the literature, there have been only a few reports of covalently crosslinked ionomer membranes. Nolte et al. covalently crosslinked a partially *N*-imidazolized sulfonated poly(ether sulfone) Victrex® ionomer with 4,4′-diaminodiphenylsulfone [28]. Kerres et al. developed a novel covalent crosslinking process in which polysulfones containing sulfinate groups within the chains were crosslinked via *S*-alkylation of the sulfinate groups with dihalogenoalkanes. The membranes showed decreased swelling in water but were brittle when dry. The brittleness was partially attributed to inflexibility as a result of crosslinking sites along the backbones of the copolymers [27,29,30].

In this paper, we describe the synthesis and crosslinking of BPS random copolymers with high degrees of disulfonation (e.g., 50% disulfonation) for reverse osmosis applications. A series of controlled molecular weight copolymers with phenolic endgroups were synthesized and further reacted with an approximately tetrafunctional epoxy reagent to produce crosslinked networks. The properties of the crosslinked membranes were evaluated in terms of three variables: curing time, number average molecular weight of the copolymers, and equivalents of epoxy with respect to terminal phenoxide groups in the copolymer (Table 3). The effects of crosslinking on RO properties such as water permeability, salt rejection and salt permeability have been investigated. The fundamental hypothesis is that controlled crosslinking will reduce water swelling and enhance salt rejection of highly charged membrane materials. It is postulated that this approach can lead to highly water permeable desalination membranes that also exhibit high salt rejection. This paper demonstrates that controlled crosslinking can produce the combined properties of reduced water swelling and enhanced salt rejection of highly charged membranes. This approach leads to highly water permeable desalination membranes that also exhibit high salt rejection.

2. Experimental

2.1. Materials

Monomer grade 4,4′-dichlorodiphenylsulfone (DCDPS) and 4,4′-biphenol (BP) were obtained from Solvay Advanced Polymers and Eastman Chemical Company, respectively, and dried under vacuum at 60 °C for 1 day prior to use. The sulfonated comonomer, 3,3′-disulfonate-4,4′-dichlorodiphenylsulfone (SDCDPS), was prepared following a previously published procedure [20,22], and dried under vacuum at 160 °C for 2 days before use. Potassium carbonate (Aldrich) was dried under vacuum at 110 °C for 1 day before use. Tetraglycidyl bis(*p*-aminophenyl)methane (Araldite MY721 epoxy resin) and triphenylphosphine (TPP) were obtained from Aldrich and used as-received. The reaction solvent *N*,*N*-dimethylacetamide (DMAc, Aldrich) was vacuum-distilled from calcium hydride, and stored over molecular sieves under nitrogen. Toluene (anhydrous, 99.8%), isopropanol (*ReagentPlus*™, 99%), *N*-methyl-2-pyrrolidinone (NMP, *ReagentPlus*™, 99%) and trimethylchlorosilane (silanizing agent) were obtained from Aldrich and used as-received.

2.2. Synthesis of a controlled molecular weight phenoxide-endcapped BPS50 copolymer

A controlled molecular weight, phenoxide-endcapped 50% disulfonated biphenol-based poly(arylene ether sulfone) (BPS50) was synthesized via nucleophilic aromatic substitution. The molecular weight of the copolymer was controlled by offsetting the stoichiometry of the monomers. A typical polymerization of a 5 kg mol^{-1} BPS50 (BPS50-5k) copolymer is provided. BP (3.102 g, 16.66 mmol), DCDPS (1.849 g, 6.44 mmol), and SDCDPS (4.824 g, 9.82 mmol) were added to a three-necked, round bottom reaction flask equipped with a mechanical stirrer, nitrogen inlet, Dean–Stark trap and a condenser. Potassium carbonate (2.649 g, 19.17 mmol) and

49 mL DMAc (to achieve 20% solids) were introduced into the flask. Toluene (24 mL, DMAc/toluene was 2/1 v/v) was added as the azeotropic reagent. The reaction mixture was refluxed at 150 °C for 4 h, and then the azeotrope was removed to dehydrate the system. The reaction mixture was gradually heated to 170 °C by the controlled removal of toluene, and then reacted for an additional 65–70 h. The viscous product was cooled to room temperature. The product mixture was filtered to remove salts. The copolymer was isolated by precipitation in isopropyl alcohol, filtered, and dried for 24 h at 70 °C under ambient pressure, and then for 24 h at 110 °C under vacuum.

2.3. Silanization of glass casting plates

A 20% (v/v) solution of trimethylchlorosilane in toluene was prepared. Clean glass plates were immersed in the solution for 2–3 min, removed, and then reacted in a convection oven for 1 h at 250 °C. The plates were cooled to room temperature and washed with acetone before use [31].

2.4. Film casting and epoxy curing

A 10 wt% solution of a phenoxide-endcapped BPS50 copolymer with various weight concentrations of MY721 epoxy resin and 2.5 wt% of TPP catalyst (based on epoxy resin weight) was prepared in NMP and stirred until a transparent homogeneous solution was obtained. The solution was cast on a silanized glass plate. The plate was inserted in a vacuum oven and heated at 100 °C for 2 h under vacuum, then at 150 °C for 15, 45 or 90 min without vacuum. After cooling to room temperature, the plate was removed from the oven and the membrane was peeled from the glass plate. Three different series of crosslinked membranes were prepared. In the first series, the copolymer weight and epoxy concentration were fixed at 5 kg mol^{-1} and 2 eq of epoxy groups per phenoxide end group on the copolymer. The crosslinking time was varied from 15, 45 and 90 min. Secondly, the epoxy concentration and curing time were held constant at 2 eq of epoxy per equivalent of phenoxide and 90 min while the copolymer molecular weight was varied from 3 and 5 kg mol^{-1}. In addition, a blend of BPS50-20k and BPS50-5k copolymers in a 30:70 wt% ratio to produce an average molecular weight of 10 kg mol^{-1} was investigated. Thirdly, a series of crosslinked membranes were prepared with a constant curing time of 90 min and copolymer molecular weight of 5 kg mol^{-1}, but with varied epoxy equivalents of 1, 2, 3 and 4 per phenoxide.

The nomenclature of the samples is defined as follows: *X*k-*Y*E-*Z*M, where *X* is the M_n of the BPS50 copolymer(s) in kilograms per mole, *Y* equals the equivalents of epoxy per phenoxide group on the ends of the copolymers, and *Z* is the curing time in minutes.

2.5. Characterization

2.5.1. Nuclear magnetic resonance (NMR) spectroscopy

^{1}H NMR experiments were conducted on a Varian Unity 400 MHz NMR spectrometer. All spectra of the copolymers and epoxy resin were obtained from 10% solutions (w/v) in DMSO-d_6 and $CDCl_3$, respectively, at room temperature. Proton NMR was used to determine the molecular weights of the copolymers and their compositions, and the functionality of the epoxy resin.

2.5.2. Fourier transform infrared (FTIR) spectroscopy

FTIR spectroscopy was used to study the crosslinking reactions of the copolymers. Measurements were recorded using a Tensor 27, Bruker FTIR spectrometer with the sample solution placed between two sodium chloride discs and with cured membranes.

2.5.3. Gel permeation chromatography (GPC)

GPC experiments were performed on a liquid chromatograph equipped with a Waters 1515 isocratic HPLC pump, Waters Autosampler, Waters 2414 refractive index detector and Viscotek 270 RALLS/viscometric dual detector. The mobile phase was NMP solvent containing 0.05 M LiBr. The column temperature was maintained at 60 °C because of the viscous nature of NMP. Both the solvent and the sample solution were filtered before introduction into the GPC system. Molecular weights were determined by universal calibration calibrated with polystyrene standards.

2.5.4. Intrinsic viscosity (IV)

Intrinsic viscosities were determined in NMP with 0.05 M LiBr at 25 °C using an Ubbelohde viscometer.

2.5.5. Gel fractions

Gel fractions of the networks were measured by placing 0.1–0.15 g of sample in DMAc and Soxhlet extracting for 48 h. After removal of the solvent by drying at 120 °C for 24 h under vacuum, the remaining mass was weighed as gel. Gel fractions were calculated by dividing the weights of the gels by the initial weights of the networks.

2.5.6. Water uptake

The membranes were immersed in deionized water for at least 48 h, then they were removed from the water, blot dried and quickly weighed. The membranes were vacuum dried at 110 °C overnight and the weights were recorded. The ratio of weight gain to the original membrane weight was reported as the water uptake (mass%).

$$\text{Water uptake}\ (\%) = \frac{W_{\text{wet}} - W_{\text{dry}}}{W_{\text{dry}}} \times 100 \qquad (1)$$

where W_{wet} and W_{dry} were the masses of wet and dried samples, respectively.

2.5.7. Volume swelling ratio

The membranes were equilibrated in deionized water for at least 48 h, then they were removed from the water and blot dried. The dimensions were measured in three directions (length, width and thickness) to calculate the wet volume. The samples were dried in a convection oven for 2 h at

80 °C. The ratio of volume gain to the original membrane volume was reported as the volume swelling ratio.

2.5.8. Differential scanning calorimetry (DSC)

Thermal transitions of the membranes were studied via DSC using a TA Instruments DSC Q-1000 at a heating rate of 10 °C min^{-1} under nitrogen. The onset temperature of the curing exotherm was used to assess the curing temperature. For experiments to determine the states of water and solvent-depressed T_gs, the samples were placed in thermally sealed, high volume DSC pans (TA Instruments) capable of withstanding pressure up to about 600 psi. Samples were cooled to −70 °C and then heated at a rate of 5 °C min^{-1} under a nitrogen atmosphere.

2.5.9. Thermogravimetric analysis (TGA)

Thermo-oxidative behavior of the cured membranes and residual solvent concentrations were measured on a TA Instruments TGA Q500. The typical heating rate was 10 °C min^{-1} in nitrogen.

2.5.10. Self-diffusion coefficient of water

Water self-diffusion coefficients were measured using a Varian Inova 400 MHz (for protons) NMR spectrometer with a 60 G cm^{-1} gradient diffusion probe [19]. A total of 16 points were collected across the range of gradient strength and the signal-to-noise ratio was enhanced by co-adding 4 scans.

2.5.11. Water permeability and salt rejection

In all experiments related to water and salt transport properties, the water was produced by a Millipore MilliQ system (Billerica, MA). Pure water permeability was measured using a high-pressure (up to 1000 psig) dead-end filtration system (Sterlitech TM HP4750 stirred cell, Sterlitech Corp., WA). The membrane size was 49 mm in diameter, and the active membrane area was 14.6 cm^2. The membrane thickness was 50–100 μm. Water permeability (P_W) was calculated from the volumetric water flux, V, per unit time, t, through a membrane of area A and thickness l divided by the pressure difference, Δp:

$$P_W = \frac{Vl}{At\Delta p} \tag{2}$$

In this study, NaCl was used for ion rejection studies. Salt rejection experiments were conducted in a dead-end system using feed solutions containing 2000 mg L^{-1} of NaCl (2000 ppm). The salt rejection (R) was calculated as

$$R\,(\%) = \left(1 - \frac{C_p}{C_f}\right) \times 100 \tag{3}$$

where C_p is the salt concentration in the permeant and C_f is the salt concentration in the feed water. Both C_p and C_f were measured with a digital conductivity meter (Oakton® CON 110, Cole Parmer, Vernon-Hills, NJ). The salt rejection data are reported at a feed pressure of 1000 psig (approximately 70 bar); the permeant pressure was atmospheric.

2.5.12. Salt permeability

Salt permeability through the polymer membranes was determined in diffusion cell studies conducted at atmospheric pressure [32]. Samples were rinsed five times with deionized water to completely remove any sorbed salt before beginning these measurements. A membrane coupon was sandwiched between two halves of a diffusion cell (effective membrane diameter was 1.5 cm). One side of the cell (i.e., the donor) was filled with 0.1 M NaCl solution. The other side of the cell (i.e., the receiver) was initially filled with pure, deionized water. Salt permeability through the membranes was determined at 25 °C by measuring the electrolytic conductivity of the receiver solution as a function of time. The salt permeability coefficient, P, was calculated using Eq. (4), which was derived by applying a transient mass balance to the diffusion cell:

$$Ln\left[1 - 2\frac{\sigma_R(t)}{\sigma_D(0)}\right]\left[-\frac{Vl}{2A}\right] = Pt \tag{4}$$

where $\sigma_R(t)$ is the salt concentration at time t in the receiver cell, and $\sigma_D(0)$ is the salt concentration in the donor cell at the beginning of the experiment (i.e., at $t = 0$). V is the volume of the donor and receiver chambers (cm^3), and in these experiments the donor and receiver volumes were both 35 cm^3, l is the membrane thickness (cm), A is the membrane area (cm^2), and P is the salt permeability (cm^2 s^{-1}).

3. Results and discussion

3.1. Synthesis of phenoxide terminated BPS50 copolymers

A series of controlled molecular weight BPS50 copolymers with phenoxide endgroups were synthesized from SDCDPS, DCDPS and biphenol by nucleophilic aromatic substitution (Fig. 1). The molecular weights of the copolymers were controlled by offsetting the stoichiometry between biphenol and the dihalides. Biphenol was utilized in excess to endcap the copolymers with phenoxide groups, so that the phenoxide groups could be further reacted in the crosslinking steps. Three copolymers with number average molecular weights (M_ns) of 3, 5 and 20 kg mol^{-1} were targeted. The degree of disulfonation was controlled by varying the molar ratio of SDCDPS to DCDPS. For all of the copolymers, the degree of disulfonation was 50%.

Fig. 2 shows the proton NMR spectrum of a copolymer with a targeted molecular weight of 5 kg mol^{-1}. The ratio of the integrals of the aromatic protons of the biphenol unit in the end group at 6.8 ppm (b) to those in the polymer repeat units at 7.7 ppm (m and i) were utilized to calculate M_n of the copolymers. As shown in Table 1, the experimental M_n values derived from both NMR and GPC are in good agreement with the targeted values. As expected, intrinsic viscosities of the copolymers increased with increasing molecular weight (Table 1). The degree of disulfonation was confirmed from the ratio of the integrals of protons at 6.95 (e), 7.8 (f) and 8.25 ppm (g) in the sulfonated unit to the protons at

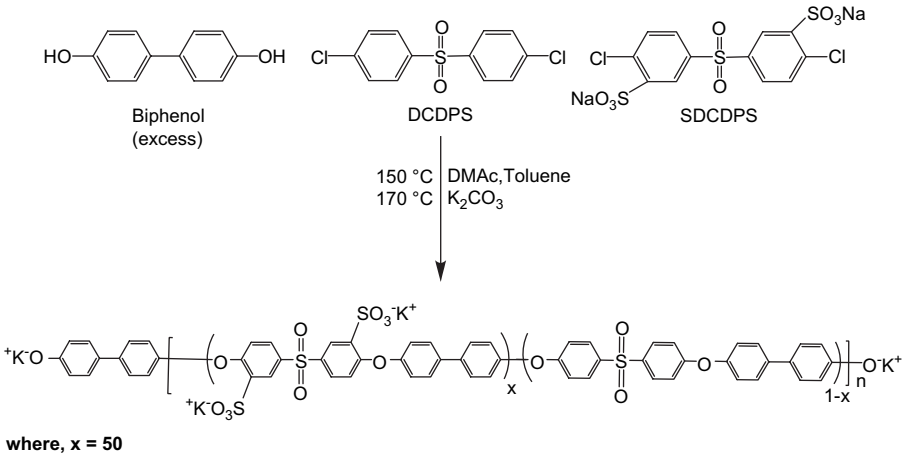

Fig. 1. Synthesis of a phenoxide-endcapped BPS50 copolymer.

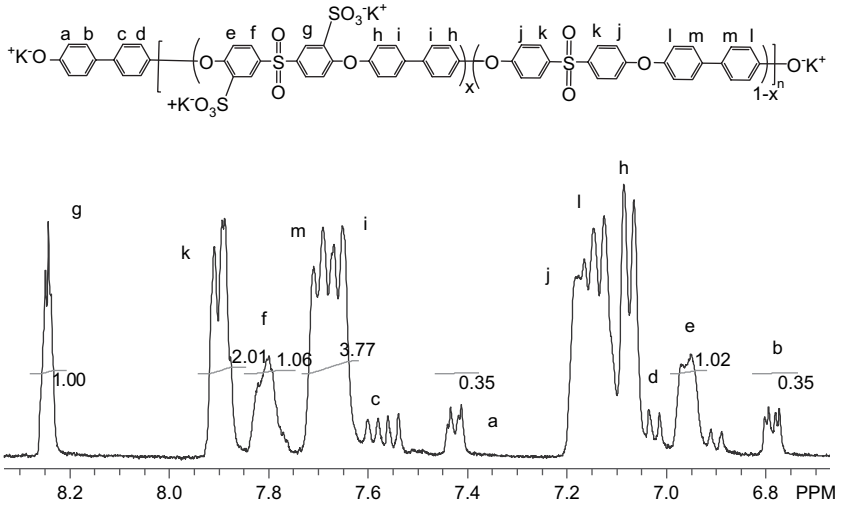

Fig. 2. ^{1}H NMR of a phenoxide-endcapped BPS50 copolymer.

Table 1
Summary of BPS50 copolymers

Copolymer	M_n (kg mol^{-1})			IV[a] (dL g^{-1})	IEC (meq g^{-1})		
	Target	^{1}H NMR	GPC		Target	^{1}H NMR	Titration[b]
BPS50-3k	3	3.5	3.6	0.16	2.08	2.08	–
BPS50-5k	5	5.8	5.2	0.22	2.08	2.04	–
BPS50-20k	20	20.8	21.8	0.43	2.08	2.03	1.90

[a] Intrinsic viscosity (IV) in NMP with 0.05 M LiBr at 25 °C.
[b] Back-titration of sulfonic acid groups.

7.9 ppm (k) in the unsulfonated unit. The degrees of disulfonation were used to calculate the ion exchange capacities (IEC – milliequivalent of sulfonic acid groups per gram of dry polymer) of the copolymers. Table 1 shows that the experimental IEC values of the copolymers are in good agreement with the targeted values.

Tetraglycidyl bis(*p*-aminophenyl)methane (Araldite MY721) was used as the epoxy crosslinking reagent. The average functionality of the epoxy was 3.66 as determined from the ratio of the integrals of epoxy ring protons (2) at 3.1 ppm to those of the methylene protons (6) at 3.75 ppm (Fig. 3).

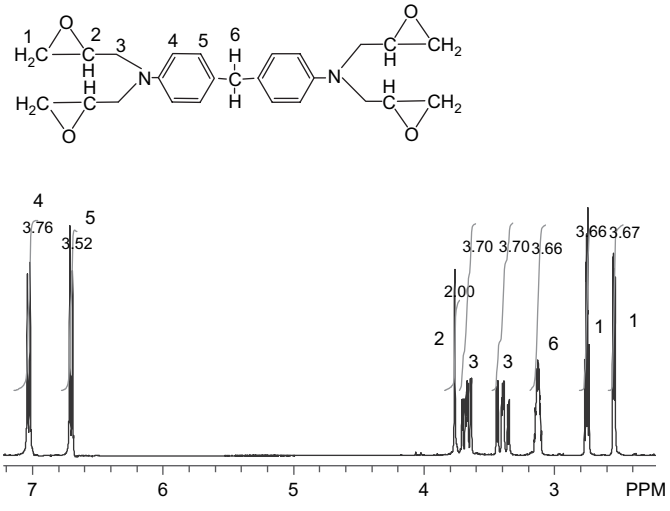

Fig. 3. ^{1}H NMR of tetraglycidyl bis(*p*-aminophenyl)methane (Araldite MY721).

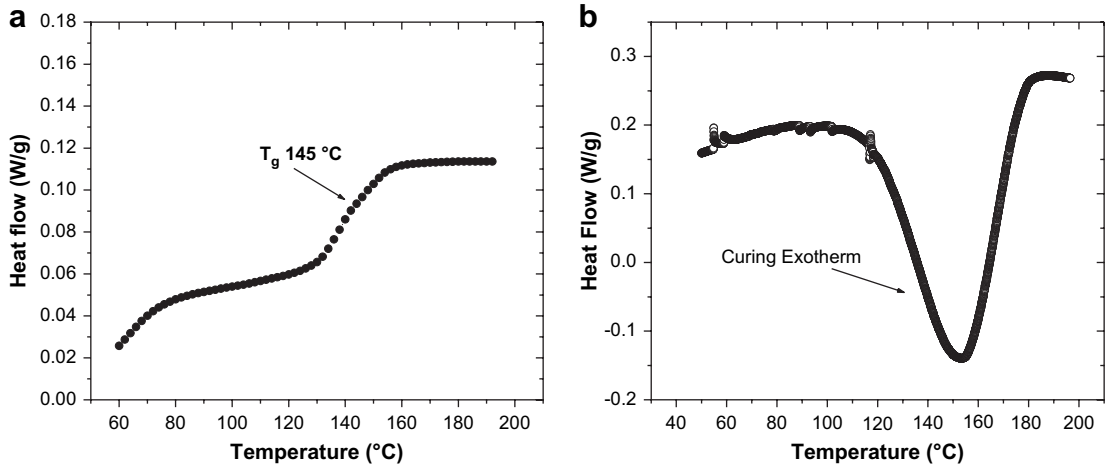

Fig. 4. (i) DSC thermogram shows solvent-depressed T_g of a BPS50 oligomer. (ii) A curing exotherm at 150 °C is observed in the DSC thermogram of an epoxy crosslinked BPS50.

3.2. Investigation of the curing reaction parameters

BPS50 is an ion-containing aromatic copolymer with a high glass transition temperature of ~250 °C. Crosslinking reactions of such a high T_g copolymer are challenging because of the need to avoid vitrification. One method for achieving high conversions is to conduct the crosslinking reaction in the presence of a high boiling solvent such as NMP so that the solvent can depress the T_g of the network as it forms. A DSC thermogram (Fig. 4(i)) of a BPS50 oligomer containing about 42% solvent (Table 2) shows a solvent-plasticized T_g of ~145 °C. Fig. 4(ii) shows a curing exotherm at ~150 °C from an epoxy-BPS50 crosslinking reaction. It is evident that the crosslinking reaction occurred above the solvent-depressed glass transition temperature. This DSC study highlights the necessity of the presence of some solvent during such crosslinking reactions. Thermogravimetric analysis (Fig. 5) was used to determine the amount of solvent that remained as a function of curing time. Table 2 shows that even after 45 min of cure, about 23 wt% solvent remained in the system. It is noteworthy that this concentration of solvent should also be sufficient for further crosslinking to take place (i.e., for membranes cured for 90 min), since it should be sufficient to depress the T_gs of networks with higher gel fractions to avoid vitrification.

The crosslinking reaction was also studied by FTIR. Araldite MY721 has an epoxide ring deformation [33] at 907 cm^{-1} which does not coincide with any peaks of the BPS50 copolymer (Fig. 6(i)). Fig. 6(ii) displays the superimposed spectra of pure epoxy, the uncrosslinked polymer–epoxy mixture (5k-2E-0M) and a crosslinked network (5k-2E-90M). Both the uncrosslinked system and the pure epoxy showed similar epoxide ring deformations at 907 cm^{-1}. However, as expected, a reduction in the peak intensity was observed upon crosslinking.

Table 2
Retention of solvent as a function of crosslinking time from TGA

Sample	Solvent (%)
5k-2E-0M	42
5k-2E-45M	23
5k-2E-90M	11

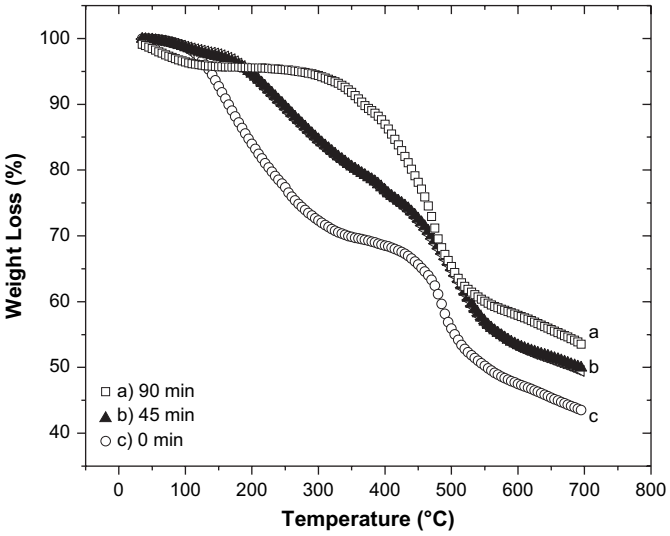

Fig. 5. TGA study showing the presence of solvent required for ongoing crosslinking reaction with increasing curing time.

3.3. Membrane properties

3.3.1. Gel fractions

Gel fractions of the crosslinked networks can be considered as an indirect measure for assessing the extent of crosslinking. As expected, the gel fractions of the cured membranes increased with increasing crosslinking time and decreasing copolymer molecular weight (Table 3). The terminal crosslinking sites increase with decreasing copolymer molecular weight. The networks formed from 2 eq of epoxy per phenoxide end group showed the highest gel fractions, whereas those with more or less than 2 eq of epoxy had lower gel fractions. There are at least two types of ring-opening reactions of the epoxies in systems of the type described herein: (1) reaction

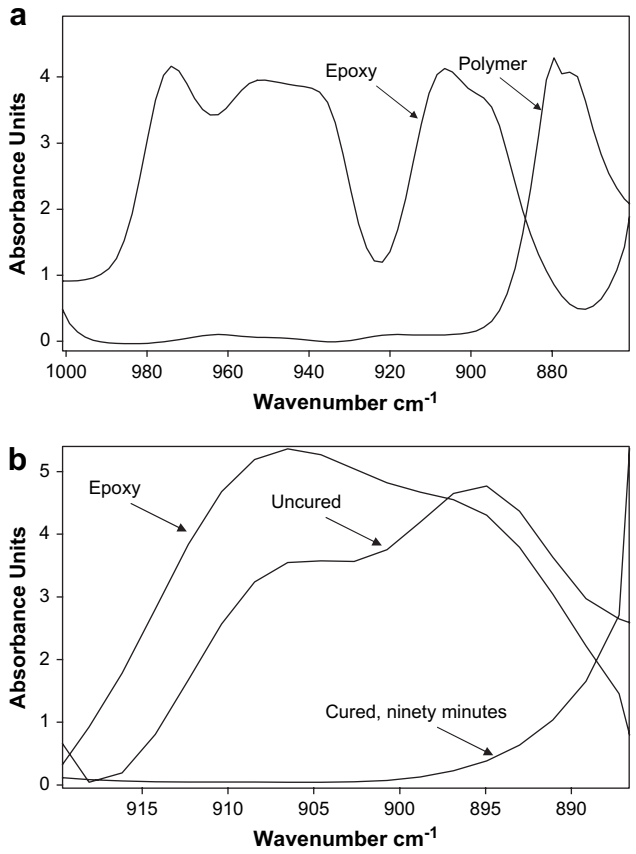

Fig. 6. FTIR spectrum showing (i) no coincidence of BPS50 copolymer peaks with epoxide ring deformation at 907 cm^{-1} and (ii) reduction in epoxide ring deformation at 907 cm^{-1} of a membrane crosslinked for 90 min.

Table 3
Properties of cured films as functions of curing time, copolymer molecular weights and epoxy equivalents

System	Curing time (min)	M_n of BPS50 (kg mol^{-1})	Equivalents of epoxy[a]	Gel fraction[b] (%) (±10%)	Water uptake (mass%) (±10%)	Swelling ratio (vol%) (±10%)
Control	0	5	0	0	51	70
5k-2E-15M	15	5	2.1	10	41	67
5k-2E-45M	45	5	2.1	20	37	50
5k-2E-90M	90	5	2.1	80	30	39
3k-2E-90M	90	3	2.1	85	34	40
5k-2E-90M	90	10	2.1	17	45	75
5k-1E-90M	90	5	1	10	45	62
5k-3E-90M	90	5	3	50	45	66
5k-4E-90M	90	5	4	9	42	48

[a] Calculated with respect to phenoxide endgroups in the polymer.
[b] Soxhlet extraction in DMAc for 48 h.

of a phenoxide end group with an epoxy group, and (2) chain extension of the epoxy reagent. Due to chain extension, 1 eq of epoxy per phenoxide end group is likely insufficient to produce high gel fractions. Although it is not yet clear exactly why approximately 2 eq of epoxy per phenoxide produces the highest gel fractions, it is reasonable that an optimum should be achieved.

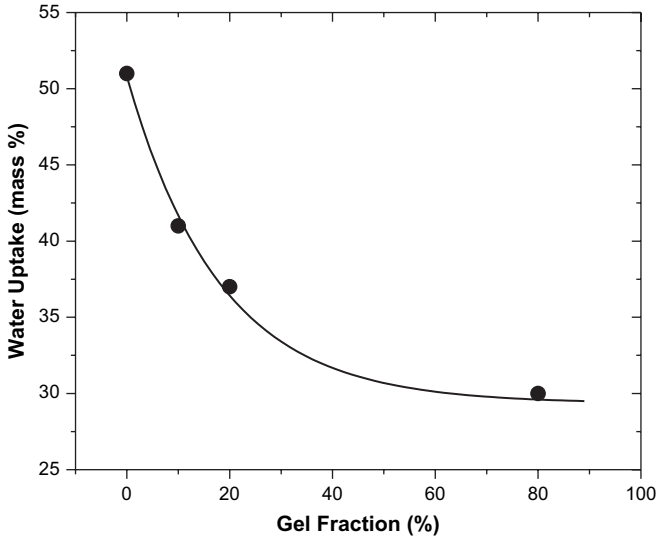

Fig. 7. Water uptake decreases exponentially as a function of gel fractions for the system with increasing curing time.

3.3.2. Water uptake and volume swelling ratio

Ion-containing polymers typically have high water uptake associated with volume swelling. This reduces the effective charge density of the membrane, and can also result in poor dimensional stability. One of the main objectives of this paper was to investigate the effect of crosslinking on water uptake and swelling of the networks. Table 3 shows a general trend of reduction in water uptake and volume swelling ratio with increasing gel fractions. The lowest water uptake and swelling were observed for the network cured with 2 eq of epoxy per phenoxide. A drastic change in water uptake and swelling occurred when the molecular weight of the copolymer was decreased from 10 to 5 or 3 kg mol^{-1}. An exponential decrease in water uptake with increasing gel fraction was found with increased curing time (Fig. 7). The highest reduction in water uptake upon curing, ~70%, was observed for the network that was cured for 90 min.

3.3.3. Self-diffusion coefficients of water

The self-diffusion coefficient of water is an intrinsic transport property of the membrane, and is related to the structure and the chemical composition of the copolymers or networks. In general, the self-diffusion coefficient of water scales with the volume fraction of the solvent or with the free volume of the system. Crosslinking of a polymer is associated with a reduction in the free volume and formation of restricted morphological structure. Self-diffusion coefficients of water were measured for the uncrosslinked and crosslinked samples. Fig. 8 illustrates the self-diffusion coefficient of water as a function of gel fractions of the networks. A significant reduction is observed at higher gel fractions relative to those for the uncrosslinked or lightly crosslinked materials. This may suggest the formation of restricted morphology and reduced water transport with increasing crosslink density.

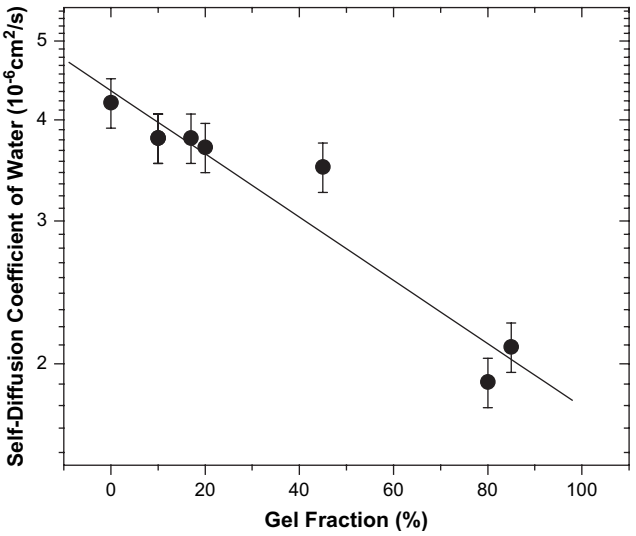

Fig. 8. Self-diffusion coefficient of water as a function of gel fractions of the cured systems.

3.3.4. States of water

There are at least three states of water that have been associated with water residing in hydrophilic phases of polymers [34–37]. The presence of these three states can be defined by thermal properties. *Non-freezing bound water* is strongly associated with the polymer and depresses its T_g, but the water shows no melting endotherm by DSC. *Freezable bound water* is weakly bound to the polymer (or weakly bound to the non-freezing water), and displays broad melting behavior at around 0 °C. *Free water* exhibits a sharp melting point at 0 °C. Earlier investigations on states of water in ion-containing polymers have shown a strong dependence of transport properties on the types of water. Fig. 9 displays the melting endotherms of the freezable water as a function of the curing time. A sharp melting peak at around 0 °C along with a broad melting endotherm is observed for the system cured for 15 min. However, the disappearance of the free water peak and a significant decrease in the area under the melting endotherm were observed for the samples cured for 45 and 90 min. The ratio of free to bound water decreases with increasing crosslinking time. Since different sites have variable interactions with water, the peaks sometimes appear asymmetric. This may be important in understanding the importance of crosslinking on fundamental transport properties. The influence of the crosslinking reaction on the hydrated T_g was also studied. The hydrated T_g increased with increasing curing time (Fig. 10).

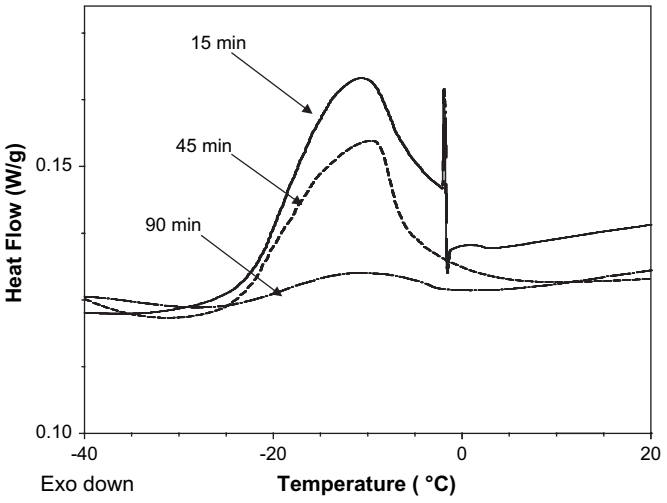

Fig. 9. DSC thermogram showing water melting endotherm peaks as a function of crosslinking time.

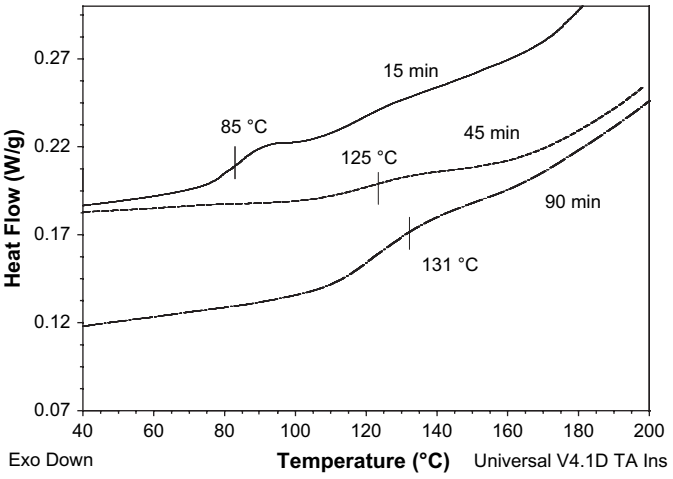

Fig. 10. DSC thermogram shows increasing hydrated T_g with curing time.

3.3.5. Water permeability and salt rejection

For reverse osmosis, membrane materials should have intrinsically high water permeability and low salt permeability. Usually, increasing the sulfonation level in sulfonated polymers increases water permeability by improving hydrophilicity, which leads to higher water uptake. However, excessive water uptake (i.e., swelling) usually increases salt passage, and also decreases mechanical properties. In addition, highly sulfonated polymers can even be soluble in water.

In negatively charged polymer membranes such as in the disulfonated polymers considered in this study, the ionic groups can electrostatically repel negative ions in solution. Therefore, the salt rejection with charged membranes can depend on charge effects as well as on various factors such as feed concentration and permeant flux. Rejection is higher at lower feed concentration due to Donnan exclusion [38–41]. Salt rejection should improve with increasing membrane charge density. For this reason, high degrees of disulfonation might improve rejection if water swelling can be controlled. Crosslinking (to reduce water swelling) of highly charged membranes (to enhance rejection) could lead to materials that are both highly water permeable and exhibit high salt rejection.

Table 4 records water permeability and sodium chloride rejection of crosslinked sulfonated polymer membranes as a function of curing time. In this table, results for the sodium sulfonate form of the polymers are reported. Increased curing time is associated with more highly crosslinked structures. For comparison, the properties of BPS50, an uncrosslinked polymer having the same sulfonic acid group concentration

Table 4
Water permeability and salt transport of crosslinked BPS copolymer films

System	Curing time (min)	Water permeability (L μm/m^2 h bar)	NaCl rejection[a] (%)	NaCl permeability[b] ($\times 10^{-8}$, cm^2 s^{-1})
BPS-5k-2E-15M	15	3.2	87.8	6.5
BPS-5k-2E-45M	45	1.5	96.1	3.8
BPS-5k-2E-90M	90	1.4	97.2	1.1
Uncrosslinked BPS50	0	3.5	73.4	–
SW30HR-380[c]	–	0.61[d]	99.7	–

[a] Feed = 2000 ppm NaCl; applied pressure = 1000 psig; temperature = 25 °C.
[b] Measured using direct salt permeability measurement (donor solution = 0.1 M NaCl).
[c] Commercial PA membrane (http://www.dow.com/liquidseps/) [42]; test conditions: feed = 32,000 mg L^{-1} NaCl; applied pressure = 800 psig; temperature = 25 °C.
[d] Unit is permeance (L/m^2 h bar).

as that found in the crosslinked samples, are also presented. As expected, water permeability decreases somewhat as the curing time was increased from 15 to 90 min, indicating that crosslinking modifies the pathway for water transport. On the other hand, the NaCl rejection increases strongly with curing time, ranging from 73.4% rejection for the uncrosslinked control to 97.2% for the crosslinked membrane cured for 90 min. Undoubtedly, changes in the material structure brought about by the thermal treatments have subtle effects that systematically reduce the water swelling of the materials. Substantial further studies will be needed to fully understand this phenomenon.

The NaCl permeabilities (cm^2 s^{-1}) of the crosslinked copolymer membranes are also sensitive to the structural changes brought about by the crosslinking reactions. The permeability decreases regularly with increasing curing time (Table 4), indicating that crosslinking effectively restrains transport of hydrated salt molecules through the sulfonated polymer films. These results suggest that covalent crosslinking of sulfonated polymers is a promising method to achieve high salt rejection, while maintaining high water permeability.

The crosslinked membranes were compared with a commercial PA membrane, FILMTEC SW30HR-380 [42], in terms of water permeability and salt rejection (Table 4). It is hard to obtain a true comparison between the salt rejections of the crosslinked and the commercial PA membrane due to the higher thickness of the crosslinked membranes and also due to the difference in testing conditions. Salt rejection of the crosslinked membranes was measured using a dead-end filtration at a higher operating pressure (1000 psig). In fact, salt rejection data derived from a dead-end filtration are usually lower than those from a cross-flow filtration because concentration polarization often occurs in the dead-end filtration, particularly under such a high operating condition (1000 psig). Salt rejection is expected to improve with thinner crosslinked membranes and further optimization of the crosslinking variables.

We have recently demonstrated that thin film composite membranes of thermoplastic random BPS copolymers having comparable selective layers (0.7–1.2 μm) as that of commercial polyamides were prepared successfully [24]. The ongoing and future plan is to implement the same strategy for preparing thin film composite membranes for crosslinked BPS systems. Additionally, the influence of crosslinking on chlorine stability of the membranes will also be determined experimentally.

4. Conclusions

A series of controlled molecular weight, 50% disulfonated poly(arylene ether sulfone)s were synthesized with phenoxide endgroups. These endgroups were reacted with a multifunctional epoxy resin to produce robust, crosslinked, hydrophilic membranes. By only crosslinking the materials at their endgroups, flexible, ductile films were achieved. In general, gel fraction increased with increasing curing time and decreasing copolymer molecular weight. It was determined that the membrane crosslinked for 90 min with 2 eq of epoxy per phenoxide end group had the highest gel fraction. All of the cured membranes had lower water uptake and swelling relative to their uncrosslinked counterparts, and less water uptake and volume swelling were correlated with increasing gel fractions.

The self-diffusion coefficients of water also decreased with increasing gel fraction, indicating restricted water transport with increased crosslinking. Salt rejection of the BPS50 copolymer improved dramatically after crosslinking. The membranes that had been cured for longer times showed 97.2% salt rejection compared to only 73.4% rejection without crosslinking, while the water permeability of the crosslinked membrane only decreased modestly. Reductions in salt permeability with increasing crosslink density also suggested that crosslinking inhibits salt transport through the membrane. The effects of crosslinking on fundamental water and salt transport properties of these highly disulfonated copolymers are encouraging and suggest their potential as candidates for RO membranes.

Acknowledgements

The authors would like to thank the Office of Naval Research (N00014-05-01-0772 and N00014-06-1-1109) and the National Science Foundation (IIP-0650277) for their support.

References

[1] Oki T, Kanae S. Science 2006;313(5790):1068–72.
[2] Service RF. Science 2006;313(5790):1088–90.
[3] Graefe AF, Wong D. NTIS report no. PB81-115420; 1980.
[4] Avlonitis S, Hanbury WT, Hodgkiess T. Desalination 1992;85(3):321–34.
[5] Knoell T. Ultrapure Water 2006;23(3):24–31.
[6] Petersen RJ. Journal of Membrane Science 1993;83(1):81–150.
[7] Allegrezza Jr AE, Parekh BS, Parise PL, Swiniarski EJ, White JL. Desalination 1987;64:285–304.
[8] Noshay A, Robeson LM. Journal of Applied Polymer Science 1976;20(7):1885–903.
[9] Plummer CW, Kimura G, La Conti AB. NTIS report no. PB-201034; 1970.
[10] LaConti AB, Chludzinski PJ, Fickett AP. In: Lonsdale HK, editor. Reverse osmosis membrane research. New York, NY: Plenum; 1972. p. 263–84.
[11] Bourganel J. DE 72-2225284, Rhone-Poulenc S.A.; 1972.

[12] Quentin JP. DE 70-2021383, Rhone-Poulenc S.A.; 1970.
[13] Schiffer DK, Davis RB, Coplan MJ, Kramer CE. NTIS report no. PB81-167215; 1980.
[14] Friedrich C, Driancourt A, Noel C, Monnerie L. Desalination 1981; 36(1):39–62.
[15] Harrison WL, Hickner MA, Kim YS, McGrath JE. Fuel Cells 2005; 5(2):201–12.
[16] Hickner MA, Ghassemi H, Kim YS, Einsla BR, McGrath JE. Chemical Reviews 2004;104(10):4587–611.
[17] Kim YS, Hickner MA, Dong LM, Pivovar BS, McGrath JE. Journal of Membrane Science 2004;243(1–2):317–26.
[18] Kinzer KE, Lloyd DR, Gay MS, Wightman JP, Johnson BC, McGrath JE. Journal of Membrane Science 1985;22(1):1–29.
[19] Roy A, Hickner MA, Yu X, Li Y, Glass TE, McGrath JE. Journal of Polymer Science, Part B: Polymer Physics 2006;44(16):2226–39.
[20] Sankir M, Bhanu VA, Harrison WL, Ghassemi H, Wiles KB, Glass TE, et al. Journal of Applied Polymer Science 2006;100(6):4595–602.
[21] Summer MJ, Harrison WL, Weyers RM, Kim YS, McGrath JE, Riffle JS, et al. Journal of Membrane Science 2004;239(2):199–211.
[22] Wang F, Hickner M, Kim YS, Zawodzinski TA, McGrath JE. Journal of Membrane Science 2002;197(1–2):231–42.
[23] Wang H, Badami AS, Roy A, McGrath JE. Journal of Polymer Science, Part A: Polymer Chemistry 2006;45(2):284–94.
[24] Park HB, Freeman BD, Zhang Z, Sankir M, McGrath JE. Angewandte Chemie International Edition, in preparation.
[25] Park HB, Freeman BD, Zhang Z-B, Fan G-Y, Sankir M, McGrath JE. PMSE Preprints 2006;95:889–91.
[26] Zhang Z-B, Fan G-Y, Sankir M, Park HB, Freeman BD, McGrath JE. PMSE Preprints 2006;95:887–8.
[27] Kerres JA. Fuel Cells 2005;5(2):230–47.
[28] Nolte R, Ledjeff K, Bauer M, Muelhaupt R. Journal of Membrane Science 1993;83(2):211–20.
[29] Kerres J, Cui W, Junginger M. Journal of Membrane Science 1998; 139(2):227–41.
[30] Kerres J, Zhang W, Cui W. Journal of Polymer Science, Part A: Polymer Chemistry 1998;36(9):1441–8.
[31] Mecham SJ. Gas permeability of polyimide/polysiloxane block copolymers. MS thesis, Chemistry, Blacksburg, VA: Virginia Polytechnic Institute and State University; 1994.
[32] Yasuda H, Lamaze CE, Ikenberry LD. Makromolekulare Chemie 1968; 118:19–35.
[33] Rocks J, Rintoul L, Vohwinkel F, George G. Polymer 2004;45(20): 6799–811.
[34] Hodge RM, Bastow TJ, Edward GH, Simon GP, Hill AJ. Macromolecules 1996;29(25):8137–43.
[35] Hodge RM, Edward GH, Simon GP. Polymer 1996;37(8):1371–6.
[36] Kim YS, Dong LM, Hickner MA, Glass TE, Webb V, McGrath JE. Macromolecules 2003;36(17):6281–5.
[37] Quinn FX, Kampff E, Smyth G, McBrierty VJ. Macromolecules 1988;21(11):3191–8.
[38] Donnan FG. Journal of Membrane Science 1995;100(1):45–55.
[39] Donnan FG, Allmand AJ. Journal of the Chemical Society Transactions 1914;105:1941–63.
[40] Tsuru T, Nakao S, Kimura S. Journal of Chemical Engineering of Japan 1990;23(5):604–10.
[41] Tsuru T, Urairi M, Nakao S, Kimura S. Journal of Chemical Engineering of Japan 1991;24(4):518–24.
[42] http://www.dow.com/liquidseps/.